Journal of Engg. Research **Vol. 6 No. (4) December 2018 pp** *1-21*

Novel Coupled Model for Productivity Prediction in Horizontal Wells in Consideration of True Well Trajectory

Wei Luo*, Ruiquan Liao*, Xiuwu Wang*, Ming Yang**, Weilin Qi*** and Zilong Liu*

**Petroleum Engineering Institute of Yangtze University, Wuhan, Hubei, 430100, China*
**Key Laboratory of Exploration Technologies for Oil and Gas Resources (Yangtze University), Ministry of Education, Wuhan, Hubei, 430100, China*
***Research Institute of Exploration and Development, Tuha Oil Field Company, PetroChina, Hami, Xinjiang 839009, China*
****Research and Development Center, Tuha Oilfield Company, Shanshan, Xinjiang, 838202, China*
**Corresponding Author: liaoruiquan@263.net*

ABSTRACT

On the basis of previous research, the true trajectory of horizontal oil wells with complex structures is considered in this study. A horizontal well is an assembly of a myriad of infinitesimal section lines along the well's length. Hence, a method to calculate the true horizontal well trajectory potential in a top-closed reservoir with bottom water is achieved. Combined with the formula of pressure drop in a single-phase variable mass flow horizontal well, a new coupled semi-analytical model for horizontal well productivity prediction is established. Using a well from an offshore oilfield in China as case study, productivity prediction via calculation and comparison of the horizontal well is conducted. Prediction results show that the new model is more accurate than other models considered. The established model for real 3D well trajectory potential converts the integral solution into even-number segments to avoid the defect of zero denominator when potential calculation is conducted for the self-infinitesimal scenario. In summary, the new coupled semi-analytical calculation model of productivity prediction for horizontal wells is built by establishing a calculation model for the true trajectory potential of a horizontal well. This model is proven feasible through actual case calculation. The new model is refined and stable, and productivity prediction under true trajectory conditions can be obtained with the new model. Such productivity prediction reflects the real situation of oil wells and is conducive for the optimal design of well trajectory and parameters.

Key words: coupled semi-analytical model; productivity prediction; horizontal wells; true trajectory; optimal design

INTRODUCTION

Similar to vertical wells, production in horizontal wells involve two processes: flowing in layers and in pipes separately. Although many similarities exist between horizontal and vertical wells, the flow process in horizontal wells is much more complicated. To understand the characteristics of horizontal well production, the two processes are usually merged during analysis. The flow in a reservoir follows the rules of seepage while flow in pipes follows the rules of variable mass flow. In order to merge the two processes for effective analyses, a coupled model must be built and a solution established. In the earlier research, many methods proposed (V. P. Merkulov, 1958; J. P.

Borisov, 1964; Giger F. M. et al., 1984; Joshi S.D. et al., 1988; Renard G. et al., 1991; Elgaghah S. A., Osisanya S. O., & Tiab D., 1996; Dou Hong'en, 1996; Economides M. J., Deimbachor F. X., Brand C. W., & Heinemann Z. E., 1991; Frick T. P. & Economides M. J., 1993) have been simplified, considering only the flow of the seepage and neglecting the effect of the flow of pipes. It is clear that a fully coupled approach is not fully considered.

Given that the structure of horizontal and multilateral wells with branches is complicated, many people have carried out related researches. Most of them (Marett et al., 1993; Ozkan et al., 1995; Popa et al., 1996; Liu Xiangping et al., 1999; Yula Tang et al., 2000; Liu Xiangping et al., 2000a; Chen Yaohui et al., 2002; Han Guoqing et al., 2004; Chen Wei et al., 2004; Li Xiaoping et al., 2005; Vicente et al., 2006; Su Yuliang et al., 2007; Mohammadsalehi et al., 2010; Zhang Lin et al., 2011; Xie Xun et al., 2012; Yuan Lin et al., 2014;) have carried out horizontal well production simulation studies and a few (Salas et al., 1996; Liu Xiangping et al., 2000b; He Haifeng et al., 2004; Fan Yuping et al., 2006; Chen Weidong et al., 2006; Yang Xiaosong et al., 2008; Yue Ping et al., 2015) have carried out multilateral well production simulation studies. Excluding a few studies (Vicente et al., 2006; Salas et al., 1996;) are simulated by simulators, other studies are carried out by using the superposition principle of potential. Some methods are superimposed by pressure, essentially superposition of potential, with some differences in form. These methods involve simulating horizontal and multilateral wells with branches as a straight line, which is unsuitable and may result in large errors in several instances, as explained in several references (Qi Zhilin et al., 2006; He Fengguo et al., 2009). Only a few methods consider the wellbore trajectory (Chen Yaohui et al., 2002; Qi Zhilin et al., 2006; Ouyang et al., 1998; Ouyang et al., 2001; Christian et al., 2000; Vicente et al., 2001; Gui et al., 2007; Kabir et al., 2009). Several studies (Chen Yaohui et al., 2002; Qi Zhilin et al., 2006) were based on the formula of Xiangping Liu (Liu Xiangping et al., 1999). During the calculation of this formula, the denominator could be zero, which is inaccurate.

Ouyang et al., (1998) and Ouyang et al., 2001 adopted the potential of the middle point of the infinitesimal section as a substitute and established a transient model of a horizontal or multilateral well. This model uses the same principle as that of Xiangping Liu (1999). No essential difference exists. Although the formula form is consistent, it is based on the superposition model of pressure that does not comply with the potential superposition principle. The study conducted by Christian et al. (2000) was an extension of the studies of Ouyang et al. (1998 and 2001). It also possesses the same shortcomings as the original model. Numerical simulations have also been conducted (Vicente et al., 2001; Gui et al., 2007; Kabir et al., 2009) by establishing partial differential equations or simulators (based on partial differential equations). Vicente et al. focused on the productivity transient simulation research of horizontal wells with various fracture parameters by establishing partial differential equations. A transient simulation of oil, gas, and water phases was carried out by establishing partial differential equations (Gui et al., 2007). Kabir et al. (ref) thought that a few semi-analytical modeling approaches by simplifying assumptions in the previous studies are less than accurate inflow profile prediction of horizontal wells through coupling of a reservoir and a wellbore simulator. However, they did not provide a reliable comparative study. Additionally, these approaches belong to the category of numerical simulations by establishing partial differential equations, and they have an important drawback, that is, the need for a large amount of simulation time. In this context and on the basis of a previous research method (Liu Xiangping et al., 1999) that used the potential superposition principle, a new model for predicting the productivity of horizontal wells with a real wellbore trajectory has been developed in this study and compared with the Liu Xiangping model.

3D STEADY SEEPAGE FLOW MODEL IN CONSIDERATION OF THE TRUE WELLBORE TRAJECTORY

The single-phase isothermal flow of a slightly compressible fluid (liquid) with constant compressibility c and μ viscosity in a horizontal well with length L in a homogeneous porous medium is considered. 2D anisotropy in the reservoir is assumed and K_h and K_v are horizontal and vertical permeability, respectively.

While there are four types of reservoirs, the top-closed reservoir with bottom water is considered. The calculation procedures employed are similar to that utilised in Liu Xiangping et al. (1999). Given that the multilateral well is an extension of the horizontal well, the 3D flow model can be used for both.

1. Calculation of the potential in true wellbore trajectory

The entire potential in point (X, Y, Z) from one horizontal wellbore which has a uniform flow can be

$$\phi = \sum_{i=1}^{m} \phi_i = -\frac{q}{4\pi L} \sum_{i=1}^{m} \left(\int_{x_{si}}^{x_{ei}} f(x, y_{si}, z_{si}) dx + \int_{y_{si}}^{y_{ei}} g(x, y, z_{si}) dy + \int_{z_{si}}^{z_{ei}} h(x, y, z) dz \right) \tag{1}$$

In the formula, ϕ is the entire potential of horizontal well in point (X, Y, Z), q is the production rate of horizontal well, m is the parts of horizontal well divided into, (x_{si}, y_{si}, z_{si}) is the start coordinate of i part, (x_{ei}, y_{ei}, z_{ei}) is the end coordinate of i part, f, (x, y, z), g (x, y, z), and h (x, y, z), are the function of x, y, z, (The detailed definitions are provided in the Appendix A).

For different areas, the directions of the inflow from the edges present several differences with the inflow from the middle side. A mutual effect exists in interfacing parts as the pressure drop appears. The flow rates of the different parts of the horizontal wellbore are different in the reservoir. Thus, the entire horizontal part is divided into many small parts because a small part is too short to be regarded as having a uniform flow. The potential created by each part can be obtained with Formula 1 (Formula A-20 in the appendix). This formula can calculate each part separately, and it is highly accurate. The derivation of this formula and the advantages are described in Appendix A.

The calculating procedure for the potential of a top-closed reservoir with bottom water is shown in the following subsection.

2. Calculation of potential from a horizontal well in a top-closed reservoir with bottom water

For the reservoir shown in Figure 1, by dividing horizontal length L into N parts, the potential can be calculated with mirror reflection theory, as shown in Figure 2.

$$\begin{aligned} \phi_j(X,Y,Z) = -\frac{q_j}{4\pi} \{ \sum_{n=-\infty}^{\infty} [\xi_j(x, y, 4nh + z, X, Y, Z) + \xi_j(x, y, 4nh + 2h - z, X, Y, Z) - \xi_j \\ (x, y, 4nh - z, X, Y, Z) - \xi_j(x, y, 4nh - 2h + z, X, Y, Z)] \} + C_j \end{aligned} \tag{2}$$

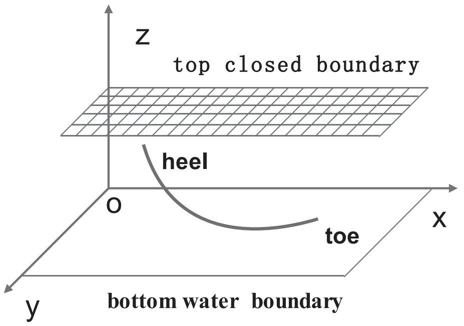

Fig. 1. Schematic of a horizontal well in a top-closed reservoir with bottom water

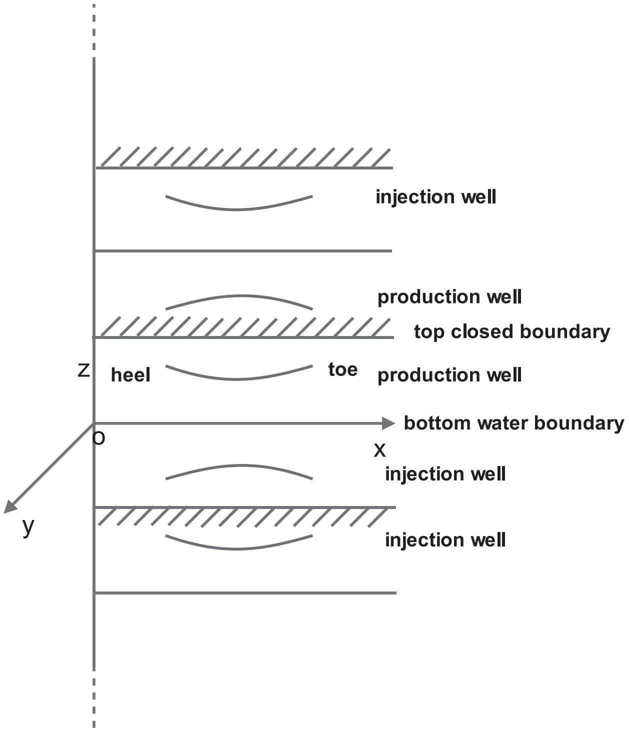

Fig. 2. Mirror image of a horizontal well in a top-closed reservoir with bottom water

In the formula, ϕ_j is the potential of part *j, q,* is the flow rate of part *j, h* is the thickness of the oil layer, *z* is the distance from the horizontal well to the bottom of the layer, C_j is a constant, and ξ is defined below.

$$\xi_j(x, y, 4nh + z, X, Y, Z) = \frac{1}{L_j}\sum_{i=1}^{m}\left(\int_{x_{jsi}}^{x_{jei}} f(x)dx + \int_{y_{jsi}}^{y_{jei}} g(y)dy + \int_{4nh+z_{jsi}}^{4nh+z_{jei}} h(z)dz\right) \quad (3)$$

where L_j is the length of part j, x_{js1} is the start coordinate, and x_{jem} is the end coordinate in direction. *X* The rest of the parameters are coordinates in *y* and directions.

3. Inflow relationship in a horizontal well

Based on the superposition principle of the potential, the entire potential of a horizontal well can be calculated.

$$\phi(X,Y,Z) = \sum_{j=1}^{N} \phi_j(X,Y,Z) + C = -\sum_{j=1}^{N} \frac{q_j}{4\pi}\varphi_j + C \tag{4}$$

From Formula 4, we have

$$\phi_e = \sum_{j=1}^{N} \phi_{je} + C, \tag{5}$$

where ϕ_e is the constant pressure of the boundary or the potential of the oil drainage boundary and ϕ_{je} is the constant pressure of the boundary or the potential of the oil drainage boundary of part j.

Combining Formulas 4 and 5 yields

$$\phi(X,Y,Z) = \phi_e + \sum_{j=1}^{N} [\phi_j(X,Y,Z) - \phi_{je}]. \tag{6}$$

According to the potential function,

$$p(X,Y,Z) = \frac{\mu}{k}\phi(X,Y,Z) - \rho g H, \tag{7}$$

where p is the pressure in the oil layer, k is the permeability, μ is the viscosity, ρ is the density, H is the height, and g is the acceleration of gravity.

Incorporating Formula 6 into Formula 7 results in

$$p(X,Y,Z) = p_e + \frac{\mu}{k}\sum_{j=1}^{N} [\phi_j(X,Y,Z) - \phi_{je}] - \rho g(Z - z_e). \tag{8}$$

In Formula 8, p_e is the boundary pressure and z_e is the coordinate in the z direction.

In consideration of anisotropy, this study selected the permeability of geometric average as $k = \sqrt{K_h K_v}$.

The rule of seepage flow is reflected by Formula 8, which denotes the relationship between the external pressure of the wellbore and inflow productivity. The rule of variable mass flow needs to be considered when building the coupled model.

MODEL OF THE FLOW IN THE WELLBORE

The process can be classified into two categories according to the completion system, as shown in Figs. 3 and 4. The first category has two types of flow processes: layer and pipe flows. The second category has three types of flow processes: layer, annular, and pipe-center flows. For ease of comparison, we begin with a simple completion verification, which is the basis for building a more complex model. This study establishes a calculation model of open hole completion, so the method in Figure 3 is selected. The formation seepage model established in this study can also be applied to Figure 4's completion mode. Figure 4's completion mode is a model that considers both the annulus and central wellbore flow. Several related studies (Valvatne, P. H., 2003; Neylon, K., et al., 2009; Luo, W. et al., 2015a; Luo, W. et al., 2015b) have also shown that both flows should be considered. As long as the wellbore flow model corresponding to Figure 4 is established, the formation seepage model can be coupled with the wellbore flow model.

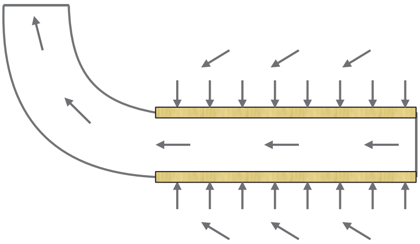

Fig. 3. First type of wellbore flow

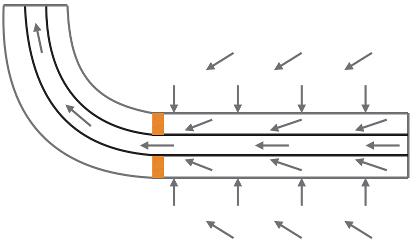

Fig. 4. Second type of wellbore flow

Many types of completion systems can be used according to the different flow processes. The first system includes barefoot and perforated completion. The second system includes central manifold completion and barefoot completion with pre-stuffed gravel in the sieve tube. This study regarded the first type as an example.

(1) Calculation model for the productivity and pressure of the infinitesimal section

Supposing that the length is *L* and the line is divided into *N* parts equally, by arranging all the parts from the start to the end, the length of each part is $\Delta X = L / N$. Part *i* is shown in Figure 5.

With $p_{1,i}$ as the up-flow pressure of part *i*, $Q_{s,i-1}$ as the up-flow productivity, $p_{2,i}$ as the down-flow pressure, and $Q_{s,i}$ as the down-flow productivity, then the pressure drop of this part $dp_{w,i}$ can be obtained as follows:

$$Q_{s,i} = Q_{s,i-1} + q_{s,i}, \tag{9}$$

$$p_{1,i} = p_{2,i} + dp_{w,i}. \tag{10}$$

The average pressure of this part is regarded as the flowing pressure, that is,

$$p_{w,i} = \frac{p_{1,i} + p_{2,i}}{2} \quad (i = 1,\ 2,\ \ldots,\ \mathrm{N}). \tag{11}$$

Supposing that the productivity of the end part is zero, that is, $Q_{s,0} = 0$, band the pressure of the start part is flowing pressure p_{wf}, we have

$$p_{wf} = p_{w,N} + \frac{1}{2} dp_{w,N}. \tag{12}$$

(2) Calculation model for pressure drop $dp_{w,i}$ in part *i*

The pressure loss of this infinitesimal part results from the loss of gravity, fractional loss, and so on. If the fractional loss is $dp_{f,i}$, then the accelerating loss is $dp_{acc,i}$, and the mixture loss is $dp_{mix,i}$. According to the principle of mass conservation, we obtain

$$\rho V_{1,i}\frac{\pi D^2}{4}+\rho V_{r,i}\pi D dx-\rho\left(V_{1,i}+\frac{\partial V}{\partial x}dx\right)\frac{\pi D^2}{4}=0. \tag{13}$$

Furthermore,

$$\frac{\partial V}{\partial x}=\frac{4V_{r,i}}{D}, \tag{14}$$

where $V_{1,i}$ is the injecting velocity of the start part in infinitesimal part i, $V_{r,i}$ is the velocity from the layer to infinitesimal part i, and D is the pipe diameter.

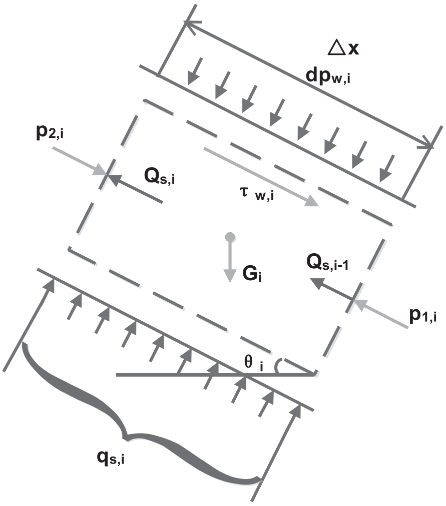

Fig. 5. Schematic of the *i* infinitesimal section

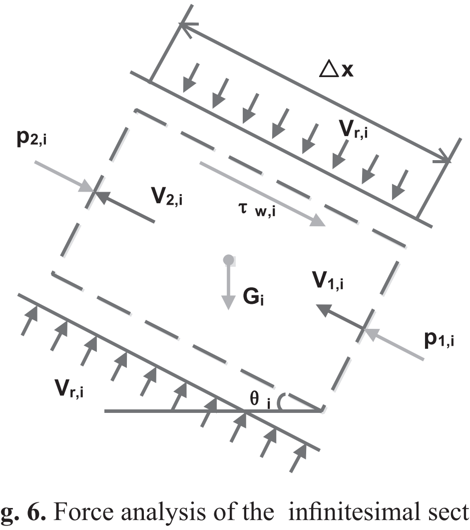

Fig. 6. Force analysis of the infinitesimal section

As shown in Figure 6, based on the conservation of momentum, pressure loss $dp_{w,i}$ can be calculated as

$$Sdp_{w,i} = mg\sin\theta_i + Sdp_{f,i} + Sdp_{acc,i} + Sdp_{mix,i} \tag{15}$$

$$dp_{w,i} = \rho\overline{V}tg\sin\theta_i + dp_{f,i} + dp_{acc,i} + dp_{mix,i} \tag{16}$$

$$-\frac{dp_{w,i}}{dx} = \rho g\sin\theta_i + \frac{4\tau_{w,i}}{D} + \rho[2V_{1,i}\frac{\partial V}{\partial x} + (\frac{\partial V}{\partial x})^2 dx] + \frac{dp_{mix,i}}{dx} \tag{17}$$

$$-\frac{dp_{w,i}}{dx} = \rho g\sin\theta_i + \frac{f_{f,i}\rho}{2D}(\frac{V_{1,i}+V_{2.i}}{2})^2 + \frac{8\rho V_{1,i}V_r}{D} + \frac{16\rho V_r^2}{D^2}dx + \frac{dp_{mix,i}}{dx} \tag{18}$$

where $dp_{w,i}$ is the pressure drop in part i, $\overline{V}$ is the average velocity of this part, t is the time to go through this part, $\tau_{w,i}$ is the wall shear stress of the pipe, $f_{f,i}$ is the frictional factor, $dp_{mix,i}$ is the mixture loss, $dp_{mix,i}$ and is considered zero for the following comparison.

COUPLED MODEL OF RESERVOIR FLOW AND WELLBORE FLOW AND THE STEADY-STATE SOLUTION

Based on the flowing situation in the pipe, the coupled model can be built with the flowing situation in the layers. Then, coordinated production can be obtained. The first type of coupled model and its solution are shown below.

The 3D seepage in the reservoir is connected with the flowing situation in the pipe, and they affect each other.

$$p_{w,j} = p_e + \frac{\mu}{k}\sum_{i=1}^{N}(\phi_{ij} - \phi_{ie}) + \rho g(z_e - z_w) \quad (j = 1, 2, \dots, N) \tag{19}$$

Formula 19 can be transformed into Formula 20.

$$\sum_{i=1}^{N}\lambda q_i(\varphi_{ij} - \varphi_{ie}) = p_e - p_{w,j} + \rho g(z_e - z_w) \quad (j = 1, 2, \dots, N), \tag{20}$$

where $\lambda = \frac{\mu}{4\pi k}$.

The pressure drop in the pipe can be calculated according to the second section. The pressure of part j is shown below.

$$p_{w,j} = p_{1,j} - 0.5dp_{w,j} \quad (j = 1, 2, \dots, N), \tag{21}$$

where $p_{2,N} = p_{wf}$ and p_{wf} is the pressure of the end point.

$$p_{1,j+1} = p_{2,j} = p_{1,j} - \Delta p_{w,j} \quad (j = 1, 2, \dots, N) \tag{22}$$

The productivity of the horizontal well is

$$Q_o = \frac{(q_{s,1} + q_{s,2} + q_{s,3} + \cdots + q_{s,N})}{B_o}, \tag{23}$$

where B_o is the oil volume factor.

Parameters q and p_w are unknown in the coupled model, and the solution can be obtained through iteration. Supposing that a series of p_w exists, q can be obtained with Formula 20, which can be incorporated into the pressure function and Formula 21 to refresh the value of q from heel to toe repeatedly until a small corresponding error exists in the values of q and p_w. Finally, productivity can be obtained with Formula 23.

MODEL CALCULATION AND VERIFICATION

Based on the data on oil wells in previous studies (Liu Xiangping et al., 1999; Fan Zifei, 1993) shown in Table 1, this study compared the outcomes of the model above and those of other models, including Xiangping Liu's model (V. P. Merkulov, 1958; J. P. Borisov, 1964; Giger F. M. et al., 1984; Joshi S.D. et al., 1988; Renard G. et al., 1991; Elgaghah S. A., Osisanya S. O., & Tiab D., 1996; Dou Hong'en, 1996; Economides M. J., Deimbachor F. X., Brand C. W., & Heinemann Z. E., 1991; Frick T. P. & Economides M. J., 1993; Liu Xiangping et al., 1999). The results are shown in Table 2. The two testing points of pressure and liquid production in the horizontal parts are shown in Figures 7 and 8, respectively. Several advantages were observed as follows.

(1) The new coupled model is more accurate than the compared ones, and the calculation of the potential is more precise. The relative error is 5.01%.

(2) The situation of zero denominator could occur in the potential calculation method of the infinitesimal section established by Liu Xiangping et al. In the calculation, if the value is large, the productivity prediction is large and vice versa. Productivity prediction was performed by taking different minimum values when the denominator is zero by using Liu Xiangping's model. A graph was drawn and is shown in Figure 9. The figure shows that Liu Xiangping's model encounters a problem. Selecting the minimum value is difficult when the denominator is zero. This value exerts a significant impact on productivity prediction, however the model established in this study can solve this problem. The value in the current study was selected by adjusting the size of the production rate of the first test points calculated by Liu Xiangping et al. The second test points were calculated on this basis. Several differences were observed between the calculated results and those of Liu Xiangping et al. The 3D model that considers the real wellbore trajectory in Formula 17 can divide the integration of the solution into even parts, thus avoiding the situation of zero denominator.

(3) The model built in this study can be used to predict the productivity in horizontal wells with real wellbore trajectory.

Results from comparisons with other models demonstrated that the new coupled model is more feasible and precise.

Table 1 Basic data on well XXX-1

Parameters	Value	Unit
Original horizontal permeability	569	mD
Original vertical permeability	280	mD
Wellbore radius	0.0549	m
Volume factor of crude oil	1.031	
Eccentricity	25.36	m
Differential pressure of testing point 1	4.57	MPa
Differential pressure of testing point 2	5.9	MPa
Drainage radius	500	m
Length of the horizontal well	599.5	m
Layer thickness	63	m
Density of crude oil	0.935	g/cm^3
Viscosity of crude oil	65	mPa.s
Production of testing point 1	1288	m^3/d
Production of testing point 2	1516	m^3/d

Table 2. Calculation results and error analysis of the methods

Method	Calculation of testing point 1 (m^3/d)	Relative error (%)	Calculation of testing point 2 (m^3/d)	Relative error (%)	Average error (%)
Merkulovb	588.31	54.3	759.52	49.9	52.1
Giger	810.67	37.1	1046.6	31.0	34.05
Joshi	575.91	55.3	743.51	51.0	53.15
Borisov	751.8	41.6	970.6	36.0	38.8
Renard	655.14	49.1	845.81	44.2	46.65
Elgaghad	617.1	52.1	796.69	47.4	49.75
Dou Hong’en	415.04	67.8	535.83	64.7	66.25
Economides*	1343.9	4.34	1735.01	14.45	9.39
Liu Xiangping	1219.25	5.34	1591.18	4.96	5.15
Proposed Method	1179.7	8.41	1540.55	1.62	5.01

* : The factor F in the formula of Economides could be a negative number if the skin factor is zero, which is very unreasonable. This formula does not consider the eccentricity of the horizontal well. For comparison, by taking the first testing point as a reference and by adjusting the skin

factor and relevant factors, the permeability of damaged zone was set as times of the original permeability. The maximum radius of damaged zone was times larger than that of the wellbore. After the adjustment, the second testing point was calculated.

The different error calculation methods in Table 2 are presented below.

The relative error is the absolute percentage error.

$$E_1 = 100 \bullet \left| e_r \right| \tag{24}$$

Where the non-absolute relative error, e_r, is given by:

$$e_r = (q_{calc} - q_{real}) / q_{real} \tag{25}$$

The average error is the absolute average percentage error.

$$E_2 = \frac{100}{N} \cdot \sum_{i=1}^{i=N} | e_{ri} \tag{26}$$

Where N is the number of test points.

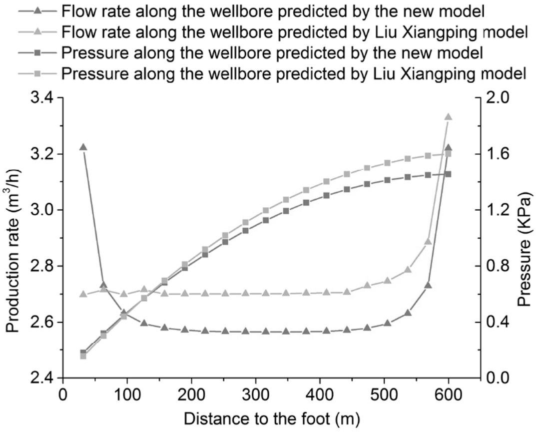

Fig. 7. Pressure and liquid production along horizontal parts in testing point 1

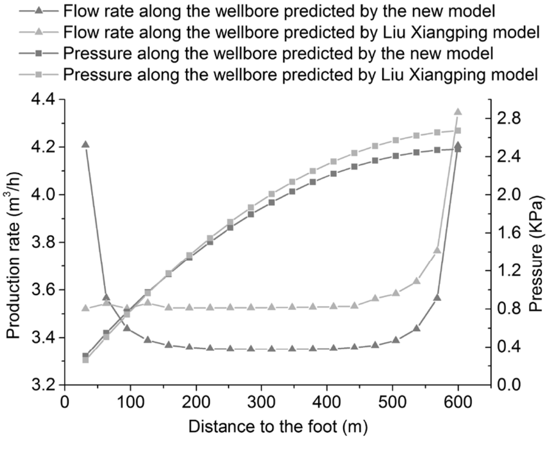

Fig. 8. Pressure and liquid production along horizontal parts in testing point 2

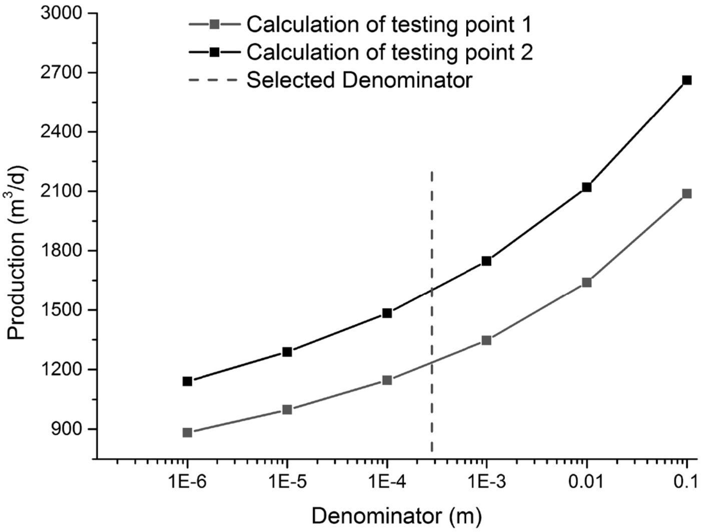

Fig. 9. Production prediction values of different denominators by using Xiangping Liu's model

With the data of oil well XXX-1 as an example, we calculated the well productivity in two different situations. In the first situation, we assumed that the bore hole is inclined, and the angle below the horizontal direction is 2°, as shown in Figure 10. In the second situation, we assumed that the trajectory of well has three coordinates, half of the bore hole is inclined, the angle below the horizontal direction is 2°, and the other half has a 1° angle below the horizontal direction, as shown in Figure 11. If the producing pressure is 4.57 MPa, the production is 1351.43 m3/d in the first situation and 1318.5 m^3/d in the second situation. The pressure and liquid production along the horizontal parts are shown in Figure 12.

Figure 12 shows that the gravity from the start to the end of the horizontal well needs to be overcome. The pressure drop in these two situations obviously increases compared with that in Figure 7. However, given that the horizontal part nearly reaches the interface of water and oil with constant pressure, the producing speed of the end part is larger than that of the start part, thus resulting in the increase in total production. Through the verification of the second situation, the true well trajectory can be calculated with the new model.

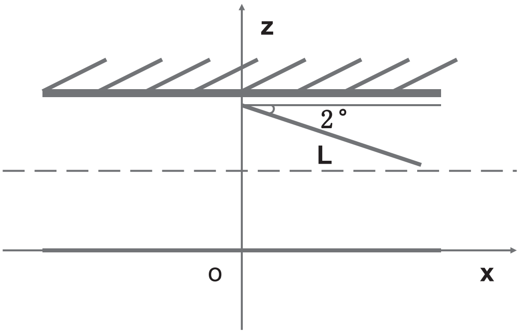

Fig. 10. First situation of the bore hole

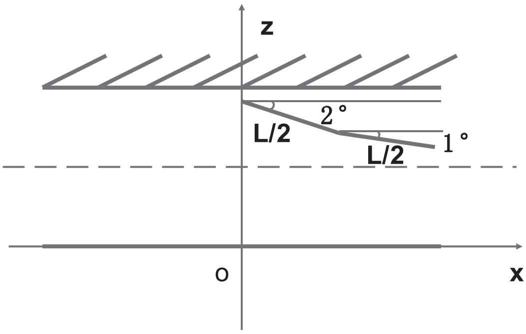

Fig. 11. Second situation of the bore hole

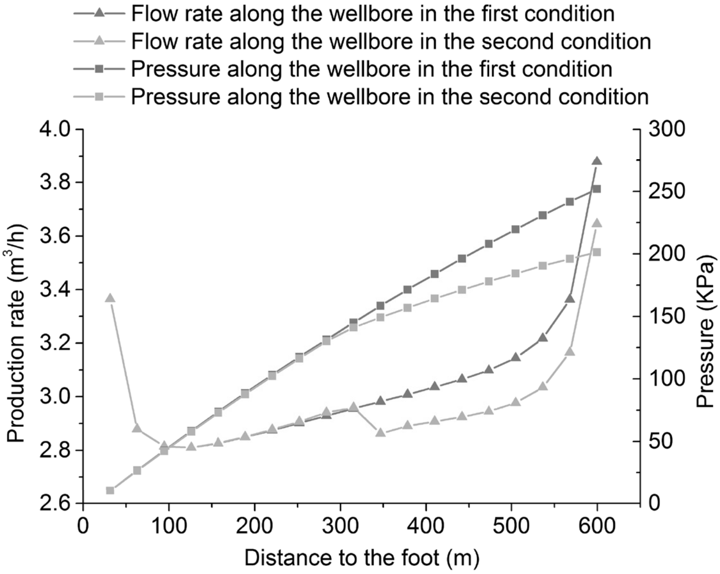

Fig. 12. Pressure and liquid production along horizontal parts in two situations

CONCLUSIONS

In this study, the following conclusions can be obtained:

(1) The new 3D coupled model is more accurate than other methods (as shown in Table. 2), and has a relative error is 5.01%.

(2) The new model is stable (The new model can divide the integration solution into even parts, thus avoiding the situation of zero denominator.) and the case caused by using Xiangping Liu method will not happen in this method (as shown in Figure 9).

(3) The new model with real wellbore trajectory is feasible. The new model can predict the productivity of a horizontal well with real wellbore trajectory and can thus reflect the effect of borehole trajectory (as shown in Figure 12). It is helpful in parameter optimization during trajectory design.

ACKNOWLEDGMENTS

Gratitude is extended to Ruiquan Liao, the corresponding author for the article. The authors would also like to acknowledge the support provided by the National Natural Science Fund Project (61572084) and major national projects (2017ZX05030–005, 2016ZX05056004–002, 2016ZX05046004–003).

APPENDIX THE CALCULATION METHOD OF HORIZONTAL WELL'S POTENTIAL

1. Calculation of the potential in true wellbore trajectory

Supposing that a point sink called M exists in space, according to the rules of seepage, the velocity of seepage can be obtained when the center is M and the spherical radius is r and the productivity is q.

$$v = \frac{q}{4\pi r^2} \tag{A-1}$$

According to the definition of "potential" and Darcy's law, the velocity of seepage can be obtained.

$$v = \frac{d\phi}{dr} \tag{A-2}$$

where $d\phi$ is the small variation of potential when the spherical radius has small variation dr.

The Formula A-1 is equal to Formula A-2.

$$\frac{q}{4\pi r^2} = \frac{d\phi}{dr} \tag{A-3}$$

By separating the formulas and by integrating, the expression of the space potential is obtained as Formula A-4.

$$\phi = -\frac{q}{4\pi r} + C \tag{A-4}$$

The 3D layer contains a horizontal well with length L and productivity q. The coordinates of the start and end parts are (x_1, y_1, z_1) and (x_2, y_2, z_2), respectively, as shown in Figure a-1. We assumed that the flow of crude oil in the layer is steady, and the horizontal well was regarded as a line sink with a uniform inflow.

After dividing the horizontal well into m parts on the average (the length of each part is L/m), the start coordinate of i part is (x_{si}, y_{si}, z_{si}), and the end coordinate is (x_{ei}, y_{ei}, z_{ei}). Additionally, $i = 1, 2, 3, \ldots m$.

After obtaining a point in one sectional part with the coordinate (x, y, z) as the final point, the length to the start point of this sectional part is

$$s = \sqrt{(x - x_{si})^2 + (y - y_{si})^2 + (z - z_{si})^2} \tag{A-5}$$

By obtaining the total differential of both sides of Formula A-5, the infinitesimal part *ds* meets the following formula.

$$ds = \frac{1}{s}[(x - x_{si})dx + (y - y_{si})dy + (z - z_{si})dz] \tag{A-6}$$

For ds , the production of this part is $dq = \frac{q}{L}ds$. The potential at point (X, Y, Z) is

$$d\phi = -\frac{dq}{4\pi r}, \tag{A-7}$$

$$d\phi = -\frac{q}{4\pi rL}ds, \tag{A-8}$$

$$d\phi = -\frac{q}{4\pi rL}\frac{1}{s}[(x - x_{si})dx + (y - y_{si})dy + (z - z_{si})dz]. \tag{A-9}$$

We supposed that $f(x, y, z,)$, $g(x, y, z,)$, and $h(x, y, z,)$, are as follows:

$$f(x,y,z) = \frac{1}{r}\frac{1}{s}(x - x_{si}), \tag{A-10}$$

$$g(x,y,z) = \frac{1}{r}\frac{1}{s}(y - y_{si}), \tag{A-11}$$

$$h(x,y,z) = \frac{1}{r}\frac{1}{s}(z - z_{si}). \tag{A-12}$$

Thus, as the spatial region belongs to 3D single connected open region G, and $f(x, y, z,)$, $g(x, y, z,)$, and $h(x, y, z,)$, have the first-order partial derivative in this region, the following formula is met.

$$\frac{\partial f}{\partial y} = \frac{\partial g}{\partial x},\ \frac{\partial f}{\partial z} = \frac{\partial h}{\partial x},\ \frac{\partial g}{\partial z} = \frac{\partial h}{\partial y} \tag{A-13}$$

The potential created by this part in space (X, Y, Z) is

$$\phi_i = \int_{(x_{si},y_{si},z_{si})}^{(x_{ei},y_{ei},z_{ei})} -\frac{q}{4\pi rL}ds + C, \tag{A-14}$$

$$\phi_i = -\frac{q}{4\pi L}\left(\int_{x_{si}}^{x_{ei}} f(x,y_{si},z_{si})dx + \int_{y_{si}}^{y_{ei}} g(x,y,z_{si})dy + \int_{z_{si}}^{z_{ei}} h(x,y,z)dz\right) + C. \tag{A-15}$$

Formula A-15 can be rewritten as

$$\phi_i = \int_{x_{si}}^{x_{ei}} -\frac{q}{4\pi rL}\frac{1}{s}(x - x_{si})dx + \int_{y_{si}}^{y_{ei}} -\frac{q}{4\pi rL}\frac{1}{s}(y - y_{si})dy + \int_{z_{si}}^{z_{ei}} -\frac{q}{4\pi rL}\frac{1}{s}(z - z_{si})dz + C \tag{A-16}$$

In the above formula, the first item on the right has x as the integration variable. y and z are constant. The rest are integrated similarly.

The first item on the right is integrated as follows:

$$\int_{x_{si}}^{x_{ei}} -\frac{q}{4\pi rL}\frac{1}{s}(x-x_{si})dx = -\frac{q}{4\pi L}\int_{x_{si}}^{x_{ei}}\frac{1}{r}\frac{1}{s}(x-x_{si})dx$$

$$= -\frac{q}{4\pi L}\int_{x_{si}}^{x_{ei}}\frac{1}{\sqrt{(x-X)^2+(y-Y)^2+(z-Z)^2}}\cdot\frac{1}{\sqrt{(x-x_{si})^2+(y-y_{si})^2+(z-z_{si})^2}}\cdot(x-x_{si})dx \quad \text{(A-17)}$$

After simplifying the formula and supposing that $a = (y - Y)^2 + (z - Z)^2$, $b = (y - y_{si})^2 + (z\text{-}z_{si})^2$,

$$= -\frac{q}{4\pi L}\int_{x_{si}}^{x_{ei}}\frac{1}{\sqrt{(x-X)^2+a}}\cdot\frac{1}{\sqrt{(x-x_{si})^2+b}}(x-x_{si})dx \quad \text{(A-18)}$$

The formula can be

$$f(x, y_{si}, z_{si}) = \frac{1}{\sqrt{(x-X)^2+a}}\cdot\frac{1}{\sqrt{(x-x_{si})^2+b}}\cdot(x-x_{si}) \quad \text{(A-19)}$$

Formula A-17 equals the integration of (x, y_{si}, z_{si}), in the domain of $[x_{si}, x_{ei}]$ then multiplied by $-\frac{q}{4\pi L}$.

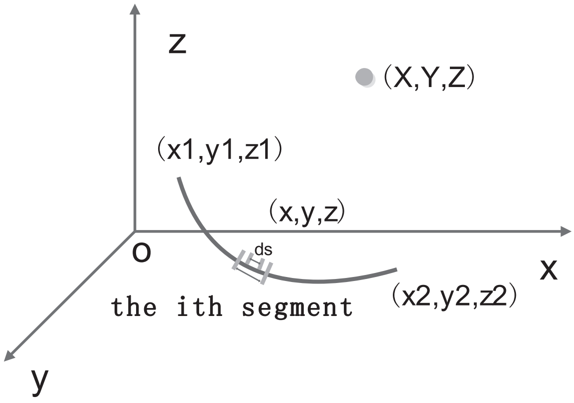

Fig. a-1. Schematic of horizontal wells in unbounded formation

Finally, the entire potential in point (X, Y, Z) from the horizontal well can be

$$\phi = \sum_{i=1}^{m}\phi_i = -\frac{q}{4\pi L}\sum_{i=1}^{m}\left(\int_{x_{si}}^{x_{ei}} f(x, y_{si}, z_{si})dx + \int_{y_{si}}^{y_{ei}} g(x, y, z_{si})dy + \int_{z_{si}}^{z_{ei}} h(x, y, z)dz\right) \quad \text{(A-20)}$$

For different areas, the directions of the inflow from the edges present several differences with the inflow from the middle side. A mutual effect exists in interfacing parts, and the pressure drop appears. The flow rates of the different parts of the horizontal wellbore are different in the reservoir. Thus, the entire horizontal part is divided into many small parts because a small part is too short to be regarded as having a uniform flow. The potential created by each part can be obtained with Formula A–20. This formula can calculate each part separately, and it is highly accurate.

2. The comparison of new method and Liu Xiangping's method

The calculation method proposed in this study is far more accurate than that of Liu Xiangping (Liu Xiangping et al., 1999). The proposed method has the following advantages. First, the proposed method segments the segmented section. Second, the formulas of the potential of a point generated by one infinitesimal section in Liu Xiangping are

$$\phi\,(x,y,z) = -\frac{q}{4\pi L}\ln\frac{r_2+(x_2-x)}{r_1+(x_1-x)}+C,\quad \phi\,(x,y,z) = -\frac{q}{4\pi L}\ln\frac{r_1+r_2+L}{r_1+r_2-L}+C.$$

Evidently, the denominator could be zero in the potential calculation of a point in the infinitesimal section self $(r_1 = x - x_1, r_2 = x_2 - x, r_1 + r_2 = x_2 - x_1 = L)$, resulting in an infinite outcome. Thus, selecting the value is difficult. If the value is too large, the production prediction would be small and vice versa. The model built in Formula A-15 can avoid this shortcoming because it addresses the subsection integral by dividing the entire trajectory into even parts. Formula A-15 can calculate the potential in any 3D point. When the potential of part *i* needs to be obtained, the formula takes the potential of middle point *i* for replacement, and the coordinate of the middle point is (*X*, 0, 0), among which $f(x,y_{si},z_{si}) = \frac{1}{\sqrt{(x-X)^2+a}}\frac{1}{\sqrt{(x-x_{si})^2+b}}(x-x_{si})$ · $\int_{x_{si}}^{x_{ei}} f(x,y_{si},z_{si})dx$ stands for integrating $f(x, y_{si}, z_{si})$ in the district of $[x_{si}, x_{ei}]$, namely, it computes the area of formula $f(x, y_{si}, z_{si})$ in the district of $[x_{si}, x_{ei}]$. By dividing the line into even parts (shown in Figure a-2), adopting the value of $f(x, y_{si}, z_{si})$, and multiplying by Δx, no zero denominator exists. When the line is divided into odd parts (shown in Figure a-3), infinite $f(x, y_{si}, z_{si})$ exists in the situation of $x = X$, similar to the calculation method of Liu Xiangping.

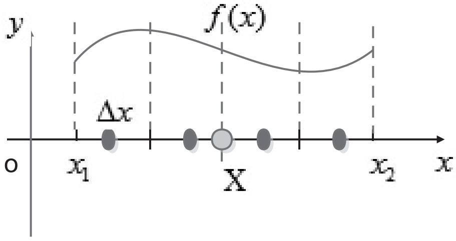

Fig. a-2. Dividing part into even segments

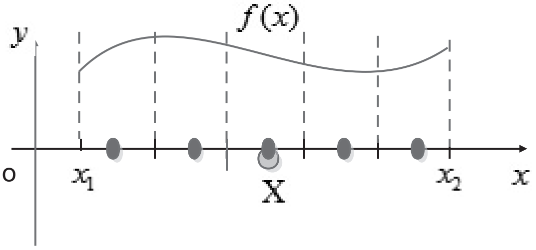

Fig. a-3. Dividing part into odd segments

REFERENCES

Chen Yaohui, Yantie, Bi Xueliang. 2002. The study of three-dimensional potential distribution theory for the reservoir of inclined well considering the wellbore pressure drop, Drilling and production technology, 05, 25–27.

Chen Wei, Duan Yonggang, Huang Cheng, Liu Qingshan, Lin Shaohong, Li Qizheng. 2004. Transient productivity prediction of bottom-water drive reservoir in horizontal well under a coupling of wellbore with reservoir, China offshore oil and gas, **16**(01), 66–69.

Chen Weidong, A. D. Hill. 2006. Development of multilateral well deliverability model, China offshore oil and gas, **18**(06), 394–398.

Christian W, Durlofsky L J, Khalid A. 2000. Approximate Model for Productivity of Nonconventional Wells in Heterogeneous Reservoirs, Spe Journal, **5**(2), 218–226.

Dou Hong'en. 1996. A new method of predicting the productivity of horizontal well, Oil Drilling & Production Technology, **18**(1), pp.76–81.

Economides, M. J., Deimbachor, F. X., Brand, C. W., & Heinemann, Z. E. 1991. Comprehensive simulation of horizontal-well performance, Spe Formation Evaluation, **6**(4), 418–426.

Elgaghah, S. A., Osisanya, S. O., & Tiab, D. 1 996. A simple productivity equation for horizontal wells based on drainage area concept, paper SPE35713 presented at the Western Regional Meeting, 22–24 May, Anchorage, Alaska.

Fan Yuping, Han Guoqing, Yang Changchun. 2006. Production forecast for herringbone well and optimum configuration of lateral holes, ACTA PETROLEI SINICA, **27**(04), 101–104.

Fan Zifei. 1993. Study for horizontal well's productivity formula in bottom-water drive reservoir, Petroleum exploration and development, **20**(01), 71–75.

Frick, T. P., & Economides, M. J. 1993. Horizontal well damage characterization and removal, Spe Production & Facilities (SPE 21795), (8):15–22.

Giger, F. M., Reiss, L. H., & Jourdan, A. P. 1984. The reservoir engineering aspects of horizontal drilling, paper SPE13024 presented at the 59th Annual Technical Conference and Exhibition, 16–19 September, Houston, Texas.

Gui, P., Cunha, L. B., & Cunha, J. C. S. 2007. A Numerical Two-Phase Flow Model Coupling Reservoir and Multi-Segment Horizontal Well, paper SPE107989 presented at the 2007 SPE Rocky Mountain Oil & Gas Technology Symposium, 16–18 April, Denver, Colorado, USA.

Han Guoqing, Wu Xiaodong, Chen Hao, Xiang-Fang, L. I., Tang, E. G., & Yong-Sheng, A. N. 2004. Influence factors for production of dual-lateral well in multilayer heterogeneous reservoirs, Journal of the university of petroleum, China, **28**(04), 81–85 .

He Fengguo, Li Liangchuan, Yue Xiangan, Zheng, J. P., & Jiang, J. L. 2009. The influence of horizontal well trajectory on recovery effectiveness of bottom water oil reservoir, Journal of southwest petroleum university (Science & Technology Edition), **31**(06), 105–109.

He Haifeng, Zhang Gongshe, Fu Xiang, Feng Guozhi. 2004. Calculating productivity of fishbone multilateral wells with nodal method, China offshore oil and gas, **16**(04), 263–265.

Joshi, S.D., et al. 1988. Production Forecasting Methods for Horizontal Wells, paper SPE17580 presented at the SPE International Meeting on Petroleum Engineering, 1–4 November, Tianjin, China.

J. P. Borisov. 1964. Oil Production Using Horizontal and Multiple Deviation Wells, The R&D Translation Company, Bartlesville, Oklahoma, USA.

Kabir A, Soto G S. 2009. Accurate Inflow Profile Prediction of Horizontal Wells through Coupling of a Reservoir and a Wellbore Simulator, paper SPE119095 presented at the 2009 SPE Reservoir Simulation Symposium, 2–4 February, The Woodlands, Texas, USA.

Liu Xiangping, Guo Chengzhu, Jiang Zhixiang, Liu Xiange, Guo Shangping. 1999. The model coupling fluid flow in the reservoir with flow in the horizontal wellbore, ACTA PETROLEI SINICA, **20**(03), 82–86.

Liu Xiangping, Zhang Zhaoshun, Liu Xiange, Guo Shangping. 2000a. A model to calculate pressure drops of horizontal wellbore variable mass flow coupled with flow in a reservoir, Journal of south-west petroleum institute, **22**(02), 36–39.

Liu Xiangping, Zhang Zhaoshun, Cui Guixiang, Wang Jialu, Yi Faxin. 2000b. Inflow performance relationship of a herringbone multilateral well, ACTA PETROLEI SINICA, **21**(06), 57–60.

Li Xiaoping, Zhang Liehui, Li Yun, & Chen, H. L. 2005. Variation laws of pressure and production rate in horizontal well, Journal of hydrodynamics, Ser. A, **20**(04), 492–496.

Luo, W., Li, H. T., Wang, Y. Q., & Wang, J. C. 2015a. A new semi-analytical model for predicting the performance of horizontal wells completed by inflow control devices in bottom-water reservoirs, Journal of Natural Gas Science & Engineering, 27, 1328–1339.

Luo, W., Li, H., Wang, Y., Wang, J., & Yang, M. 2015b. Optimization of the number of openhole packers in horizontal wells completed by inflow control devices for different types of reservoirs, Journal of Engineering Research, **3**(1), 30–41.

Marett B P, Landman M J. 1993. Optimal perforation design for horizontal wells in reservoirs with boundaries, paper SPE25366 presented at the SPE Asia Pacific Oil & Gas Conference & Exhibition, 8–10 February, Singapore.

Mohammadsalehi M, Goodarzian S and Assef M R. 2010. Non-Uniform Slotted Liner Completion, a New Approach to Obtain Uniform Production Profile along Horizontal Wells, paper SPE130219 presented at the IADC/SPE Asia Pacific Drilling Technology Conference and Exhibition, 1–3 November, Ho Chi Minh City, Vietnam.

Neylon, K., Reiso, E., Holmes, J., Nesse, O. B. 2009. Modeling well inflow control with flow in both annulus and tubing, paper SPE118909 presented at the 2009 SPE Reservoir Simulation Symposium, 2–4 February, The Woodlands, Texas, USA.

Ouyang L B, Aziz K. 1998. A Simplified Approach to Couple Wellbore Flow and Reservoir Inflow for Arbitrary Well Configurations, paper SPE48936 presented at the SPE Annual Technical Conference and Exhibition, 27–30 Sept, New Orleans, Louisiana, USA.

Ouyang L.B., Aziz K. 2001. A general single-phase wellbore/reservoir coupling model for multilateral wells, SPE Res. Eval. Eng. **4**(4), 327–335.

Ozkan E, Sarica C, Haciislamoglu M, & Raghavan, R. 1995. Effect of Conductivity on Horizontal Well Pressure Behavior, SPE Advanced Technology Series (SPE24683), **3**(01), 85–94.

Popa C G, Simion F C. 1996. A New Completion Technology to Improve Horizontal Well Performances, paper SPE37111 presented at the 2-nd International Conference on Horizontal Well Technology, 18 November, Calgary, Alberta, CANADA.

Qi Zhilin, Du Zhimin, Tang Yong, Deng, R. J., & Yan, W. D. 2006. Steady state productivity model of snaky wells, Petroleum exploration and development, **33**(01), 87–90.

Renard, G., & Dupuy, J. M. 1991. Formation damage effects on horizontal-well flow efficiency (includes associated papers 23526 and 23833 and 23839), Journal of Petroleum Technology, **43**(7), 786–869.

Salas J R, Clifford P J, and Jenkins D P. 1996. Multilateral well performance prediction, paper SPE35711 presented at the Western Regional Meeting, 22–24 May, Anchorage, Alaska.

Su Yuliang, Zhang Dong, Li Mingzhong. 2007. Mathematical model coupling Seepage in the reservoir with flow in the horizontal wellbore, Journal of China university of mining and technology, **36**(6), 752–758.

Valvatne, P. H., Serve, J., Durlofsky, L. J., & Aziz, K. 2003. Efficient modeling of nonconventional wells with downhole inflow control devices, Journal of Petroleum Science & Engineering, **39**(1–2), 99–116.

Vicente, R., Sarica, C., & Ertekin, T. 2001. A Two-Phase Model Coupling Reservoir and Horizontal Well Flow Dynamics, paper SPE69570 presented at the SPE Latin American and Caribbean Petroleum Engineering Conference, 25–28 March, Buenos Aires, Argentina.

Vicente R, Ertekin T. 2006. Modeling of coupled reservoir and multifractured horizontal well flow dynamics, paper SPE101929 presented at the 2006 SPE Annual Technical Conference and Exhibition, 24–27 September, San Antonio, Texas, USA.

V. P. Merkulov. 1958. Le debit des puits devies et horizontaux, Neft. Khoz., **6**(1), pp. 51–56.

Xie Xun, Huang Bingjia. 2012. Study on coupling model of horizontal well in bottom-water drive reservoir, Journal of Qingdao university (E&T), **27**(02), 61–65.

Yang xiaosong, Liu Chuanxi, Yan Jin, Wang, W., Shi, Z., & Jia, Y. 2008. Research on productivity law of herringbone multilateral gas well, ACTA PETROLEI SINICA, **29**(05), 727–733.

Yuan Lin, Li Xiaoping, Zhang Jiqiang, & Cheng, Z. 2014. Law of pressure drop along the horizontal wellbore in heavy oil reservoir, Lithologic reservoirs, **26**(06), 115–119.

Yue Ping, Du Zhimin, Chen Xiaofan, Fei, M., & Wei, L. 2015. A coupling model of fishbone multilateral horizontal well in bottom water reservoir, Journal of southwest petroleum university (science & technology edition), **37**(04), 117–126.

Yula Tang, Erdal Ozkan, Mohan kelkar, Cem, S., & Turhan, Y. 2000. Performance of Horizontal Wells Completed with Slotted Liners and Perforations, paper SPE65516 presented at the 2000 SPE/Petroleum Society of CIM International Conference on Horizontal Well Technology, 6–8 November, Calgary, Alberta, Canada.

Zhang Lin, Xiong Youming, Chen Yang, Xu Jianian, Liu Liming. 2011. A new reservoir flow coupling model for productivity prediction in segregated completion horizontal wells, Oil drilling and production technology, **33**(05), 24–28.

Submitted: 20/08/2017
Revised : 22/03/2018
Accepted : 18/04/2018

حديث نموذج قارن متوقع لقدرة انتاج البئر الأفقي بمسار البئر الدقيقي

لوه وي* ، لياو ريتشوان* ، وانغ شيوى وو* ، يانغ مينغ ، تشى وي لين*** و ليو تسى لونغ***

*كلية الهندسة البرولية لجامعة تشانغجيانغ ووهان هوبى الصين الشعبية 430100

*مختبر مهم لقسم تعليم تقنيات موارد وتنقيب النفط والغاز بجامعة تشانغجيانغ ووهان هوبى الصين الشعبية 430100

**معهد تنمية التنقيب لفرع شركة حقل توها البترولي الصينية هامى شينجيانغ الصين الشعبية 839009

***معهد التقنيات الهندسية لفرع شركة حقل توها شانسان شينجيانغ الصين الشعبية 838202

الخـلاصة

هذه المقالة على أساس الدراسة التاريخية ، باعتبار المسار الدقيق للبئر الأفقي بالهيكل المعقدة . البئر الأفقي هو تجمع خط التقسيم بالحد الأدنى بكبيرة الكمية لطول البئر الأفقي . لذلك ، قد يمكن حساب المسار الدقيقى لبئر أفقي بما يحتوى على طبقة ختم النفط بماء القاع . ارتباط بصيغة هبوط الضغط بئر أفقي سائل الجودة بانتجاه فردى ، تم انشاء نموذج شبه تحليلي حديث اقترانى بمتوقع قدرة انتاج البئر الأفقي . المثال ببئرما فى حقول نفط بحري فى الصين ، تم اجراء توقع قدرة الإنتاج عبر تعداد ومقارنة البئر الأفقي ، تعرض نتيجة التوقع أن النموذج الحديث أكثر دقة من النماذج الأخرى . سيحوّل نموذج الحساب لإمكانية مسار بئر 3D الحقيقى الى قطعة أرقام زوجية ، لتجنب عيوب القاسم بصفر عند تعداد الإمكانية فى حالة سيناريوهات اللانهائية . على كل حال ، تم تشكل نموذج شبه تحليلي اقترانى لتوقع قدرة انتاج البئر الأفقي الحديث عبر انشاء نموذج تعداد امكانية مسار حقيقى لبئر أفقي . على أساس حسابات الحالة الفعلية ، قد ثبت جدوى النموذج هذا . صائب ودقيق الجديد النموذج ، ممكن استخدام هذا النموذج بتوقع قدرة الإنتاج فى ظروف دقة المسار . هذا النوع من توقع قدرة الإنتاج يعكس الحالات الفعلية للحقول ، ويساعد على تحسين تصميم مسار البئر ومعلماته .

الكلمات المفتاحية : نموذج شبه تحليلي اقتراني ؛ توقع الإنتاج ؛ بئر أفقي ؛ مسار حقيقي ؛ تحسين تصميم.